JBC Papers in Press. Published on April 1, 2019 as Manuscript RA119.007527
The latest version is at http://www.jbc.org/cgi/doi/10.1074/jbc.RA119.007527

**Short title:** Collapse of Proteostasis by Tau Aggregation

# Tau protein aggregates inhibit the protein-folding and vesicular trafficking arms of the cellular proteostasis network

Anan Yu[1], Susan G. Fox, Annalisa Cavallini[2], Caroline Kerridge[2], Michael J. O'Neill[2], Joanna Wolak[2], Suchira Bose[2] and Richard I. Morimoto[1]*

**Author affiliations:**

[1]Department of Molecular Biosciences, Rice Institute for Biomedical Research, Northwestern University, Evanston, Illinois, USA, 60208
[2] Eli Lilly & Co Ltd, Lilly Research Centre, Erl Wood Manor, Sunninghill Road, Windlesham, Surrey, UK GU20 6PH

***Corresponding author:**
Richard I. Morimoto
Dept. of Molecular Biosciences
Rice Institute for Biomedical Research
Northwestern University
2205 Tech Drive, Hogan 2-100
Evanston, IL 60208
Tel: 847-491-3340
Fax: 847-491-4461
E-mail: r-morimoto@northwestern.edu

**Keywords:** tau, protein aggregation, molecular chaperones, HSC70, HSP70, HSP90, HSP110, HSP27, clathrin-mediated endocytosis, chaperone competition, human cells

## Abstract

Tauopathies are a diverse class of neurodegenerative diseases characterized by the formation of insoluble tau aggregates and the loss of cellular function and neuronal death. Tau inclusions have been shown to contain a number of proteins including molecular chaperones, but the consequence of these entrapments are not well established. Here, using a human cell system for seeding-dependent tau aggregation, we demonstrate that the molecular chaperones heat shock cognate 71 KDa protein (HSC70)/heat shock protein 70 (HSP70), HSP90, and J-domain co-chaperones are sequestered by tau aggregates. By employing single-cell analysis of protein folding and clathrin-mediated endocytosis (CME), we show that both chaperone-dependent cellular activities are significantly impaired by tau aggregation and can be reversed by treatment with small-molecule regulators of heat shock transcription factor 1 (HSF1) proteostasis that induce the expression of cytosolic chaperones. These results reveal that the sequestration of cytoplasmic molecular chaperones by tau aggregates interferes with two arms of the proteostasis network, likely having profound negative consequences for cellular function.

## Introduction

The cellular pathology of protein misfolding diseases is initiated by highly aggregation-prone proteins that can convert to oligomeric species with a propensity to form aggregates and amyloids (1-4). To prevent proteotoxic stress, cells have evolved the proteostasis network (PN), a protein quality control system that regulates and balances protein synthesis, folding, transport, and degradation (5-7). The robustness of the PN determines and maintains a balanced proteome against challenges by exposure to cell stress conditions, the chronic expression of highly aggregation-prone proteins and during aging (8,9). Non-productive interactions between protein aggregates and the protein quality control machinery impairs PN function and cellular health (10-15). A feature observed in many diseases of protein aggregation are deleterious effects on different arms of the PN (13,16-22). For example, in cells expressing either mutant huntingtin, ataxin-1 or SOD-1, the respective protein aggregates have been shown to sequester the chaperone HSC70 resulting in inhibition of clathrin-mediated endocytosis (CME) (23). This suggests that the collapse of the cellular PN occurs when chaperones such as HSC70 are sequestered by these protein aggregates and interfere with chaperone-dependent cellular activities.

Our study examines whether tau likewise interferes with the functional properties of molecular chaperones. Tau is an intrinsically disordered protein that upon mutation and post-translational modifications can adopt alternate non-native states that are highly aggregation-prone (24-29). Tau aggregation is associated with ~20 neurodegenerative diseases including Alzheimer's Disease (AD), Frontal Temporal Dementia with Parkinsonism linked to chromosome 17 (FTDP-17) and Pick's Disease (30-32). Hyperphosphorylated tau can form soluble oligomers and intracellular fibrillar inclusions known as neurofibrillary tangles (NFTs) which contain paired helical filaments of tau (25,33). Tau can generate altered conformational states that can be propagated by seed-dependent recruitment of native tau (34,35). Tau pathology in AD has been shown to spread

by cell-to-cell transmission of insoluble tau seeds as well as by amplification of tau inclusions upon seeding between brain regions (34-43).

At the cellular level, tau aggregation is affected by cytoplasmic chaperones including HSC70, HSP90 and HSP27 (44-51). Elevated levels of HSC70 suppress the formation of NFTs by redirecting tau into productive folding pathways to prevent aggregation in tissue culture cells (44). *In vitro* studies have demonstrated that tau isoforms can interact with a subset of the chaperone network to assist proper folding and prevent misfolding and aggregation (50,52-54). The interactions between chaperones with tau aggregates have also been observed in brain tissues from AD patients (44), and are supported by proteomic analysis of NFTs from tissue samples (55,56).

Tau, as for many other highly aggregation-prone proteins in neurodegenerative diseases and other protein conformational diseases, would therefore be predicted to interfere with many cellular processes. To directly examine how sequestration of key PN components by tau aggregates compromises the cellular capacity to detect, respond and protect against proteotoxicity, we have employed single-cell based cellular assays that monitor the functional properties of the PN for protein folding and clathrin-mediated vesicular trafficking using the well-established human HEK293 cell model for tauopathy (57). This cell-based tau aggregation model is dependent upon seeding with tau fibrils and amplification *in vivo* and provides an opportunity to directly compare different populations of tau aggregating species within the same experiment as determined by the recognition properties of the well-characterized antibodies MC1 and PG5 (58-64). PG5 recognizes phosphorylated serine 409 in tau and reacts specifically with the neurofibrillary tangles in AD but not normal brains, whereas MC1 antibody detects an early marker of tau pathology that corresponds to disease-specific conformational modifications of tau. Together, these reagents provide a single cell approach to examine the interaction of different tau aggregate species with cytoplasmic molecular chaperones and the consequence of these interactions on the functionality of specific arms of the proteostasis network. Our results reveal that tau aggregation inhibits the chaperone regulated PN processes of clathrin-mediated vesicular trafficking and protein folding in the cytoplasm that can be prevented and/or restored by small molecules that induce the expression of these cytoplasmic chaperones.

## Results

### Sequestration of molecular chaperones by tau aggregates

The HEK293 cell system was used for tau seeding amplification because of their low endogenous expression of various tau isoforms, thus rending these cells ideal for the conditional expression of tau (57). Protein quantitation with total tau antibody confirmed that the basal level of tau in HEK293 cells prior to tetracycline induction is 0.70 ng/µg total protein, which upon conditional expression of mutant tau P301S achieves a steady-state level of 13.8 ng/µg total protein in HEK293 tau P301S cells (Fig. S1, a-f, quantified in panel g). By comparison, iPSC derived neurons express tau at 1.5 ng/µg total protein and rat cortical neurons express tau at 4.35 ng/µg total protein, respectively.

The HEK293 cell model for tau seeding and amplification is a two-component system in which the appearance of tau inclusions is absolutely dependent upon the conditional expression of mutant 1N4R tau and simultaneous exposure to sarkosyl-insoluble tau seeds derived from the brains of TgP301S mice. Tau inclusions were detected using MC1 antibody that has been shown to recognize conformationally altered tau (Fig. S1m, arrowheads) (58-60) and PG5 antibody that recognizes late-stage hyperphosphorylated tau aggregates (Fig. S1m, arrows) (61,62). Neither expression of mutant, wild-type tau nor seeding alone resulted in detectable aggregation phenotypes (Fig. S1 h-l). PG5 and MC1 positive cells were observed only following incubation with sarkosyl-insoluble tau seeds and expression of mutant tau P301S, such that at day 3 post seeding, 6.1% of the tau expressing cells had aggregates positive for MC1 and 2.6% were positive for both MC1 and PG5 (Fig. S1n).

To examine the effects of tau aggregation on the subcellular localization of molecular chaperones, we examined individual cells by immunostaining (Figs. 1 and 2) with antibodies specific to components of the cytoplasmic Hsp70 machine (HSC70, HSP70, DNAJB1, HSP110), HSP90 and HSP27. In cells expressing MC1-positve dispersed and diffused tau, the subcellular localization of HSC70 was unaffected (Fig. 1A b and c, arrowheads), whereas HSC70 localization was altered in PG5-positive cells and co-localized with PG5 tau aggregates (Fig. 1A a and c, arrows, overlay enlarged in panel e) that were also MC1 positive (Fig. 1A b, arrows). Inducible HSP70 also co-localized with MC1 and PG5 positive tau aggregates (Fig. 1A h and l, arrows, overlay enlarged in j and n) and was associated with elevated levels of HSP70. We quantified the colocalization between different tau conformational species and HSC70 or HSP70 using Pearson correlation coefficient (PCC) (Fig. 1B). For example, PG5 positive tau inclusions and HSC70 exhibited a PCC value of 0.66 indicating a high correlation of co-localization, whereas a lower PCC value of 0.34 was observed for MC1 positive tau species and HSC70. Similarly, using a different antibody that recognizes both HSC70/HSP70, we observed a strong colocalization correlation between PG5 positive tau inclusions and (PCC value of 0.67) (Fig. 1B) relative to MC1 (PCC of 0.07). Similar patterns of colocalization between PG5 tau inclusions and inducible HSP70 (anti HSP70 antibody, clone 4G4) was observed with a PCC value of 0.62.

These observations suggest that MC1 positive tau interacts transiently with HSC70 or HSP70 with a much lower level of sequestration than observed for the PG5/MC1 positive tau inclusions that form stable sequestered interactions with these chaperones. This also suggests that stable interactions with chaperones occurs in the transition between conformationally altered diffuse tau detected by MC1 antibody and the PG5/MC1 specific tau inclusion species.

In the case of constitutively expressed HSC70, we observed a 40% increase in the levels of this chaperone in MC1 positive cells, and a 9% decrease in PG5/MC1 positive cells ($p < 0.1$) (Fig. S2A). When using an antibody that specifically recognizes HSP70, we observed a 2-fold increase in HSP70 content in PG5/MC1 cells compared to negative control cells (Fig. S2B). These results indicate that the expression of inducible HSP70 occurs after the appearance of PG5 tau inclusions.

The effects of tau on the subcellular localization of other cytoplasmic molecular chaperones was also examined in PG5/MC1 and MC1 positive cells (Fig. 2A) for DNAJB1 (Fig. 2A a-e), HSP90β (Fig. 2A f-j) and HSP110 (Fig. 2A k-o). All three chaperones are sequestered in tau aggregates in PG5/MC1 positive cells (Fig. 2A c, h and m, arrows; merged display between PG5 tau aggregates and chaperones in the boxed area enlarged in Fig. 2A e, j and o) and not altered in MC1-only cells (Fig. 2A c, h and m, arrowheads). We then examined the subcellular localization of the inducible chaperones HSP27 and HSP90α upon tau aggregation (Fig. 2B). Both HSP27 (Fig. 2B p-t) and HSP90α (Fig. 2B u-y) were likewise preferentially sequestered by tau aggregates only in PG5/MC1 positive cells (Fig. 2B r and w, arrows, overlay enlarged in t and y), with no obvious change in protein expression or subcellular localization detected in the MC1-only cells (Fig. 2B r and w, arrowheads).

Our analysis of chaperone interactions with tau inclusions indicate that multiple classes of constitutive and inducible cytoplasmic chaperones are sequestered by PG5/MC1 inclusions but to a much lesser extent with MC1-only positive inclusions. The balance between chaperone expression and their interactions with misfolded and/or aggregated tau species therefore determines the available pool of chaperones for interaction with other protein clients. Recognizing that chaperones are essential to the functional properties of the proteostasis network (PN), we next examined the consequence of sequestration of chaperones on cellular function.

**Inhibition of clathrin-mediated endocytosis in cells expressing tau aggregates**

HSC70-dependent clathrin-mediated endocytosis (CME) was monitored using a single cell-based assay that quantifies transferrin uptake by the transferrin receptor as a functional measure of CME. The seeding-dependent amplification of tau aggregate assay provided a number of important controls, that tetracycline-induced expression of either wild type (Fig. S3 b and e) or mutant tau (Fig. S3 c and f) does not affect the kinetics of transferrin uptake compared to mock treated cells (Fig. S3 a and d). Likewise, that incubation with insoluble tau seeds without conditional expression of mutant tau P301S, or with wild type tau expression also had no effect on CME (Fig. S3, quantified in panel g).

The effect of tau aggregation on CME was demonstrated in tau P301S expressing cells following seeding. PG5/MC1 positive cells (Fig. 3a, arrows) and MC1 positive cells (Fig. 3b, arrowheads) both showed reduced levels of transferrin uptake (Fig. 3c). In MC1 cells, transferrin uptake declined by 60% compared to control cells, and this corresponded to a 49% decline in PG5/MC1 positive cells (Fig. 3i). As expected, cells that were negative for both PG5 and MC1 showed the same level of transferrin uptake as untreated control cells (Fig. S3g, P301S-tet-S group). This suggests that MC1 inclusions inhibit CME to a level similar to that in PG5 positive cells despite the lower levels of chaperone interaction. The inhibition of CME in PG5/MC1 cells is associated with the appearance of tau aggregates as the levels of total tau remained unaltered from PG5 negative control cells (Fig. 3 e-h) as detected by the anti-total Tau (clone HT7)

antibody (Fig. 3f, arrows). Further, to demonstrate that CME inhibition was not a result of fluctuation in the levels of cell surface-localized transferrin receptors, we performed transferrin loading assays at 4°C to show that equivalent levels of transferrin binding to surface receptors were detected in PG5/MC1 positive cells and MC1 positive cells relative to negative control cells (Fig. S3 j and n).

**Effects of tau aggregation on cytoplasmic protein folding**

Molecular chaperones have a central role in regulating protein conformation by co- and post-translation folding to the native state, and a holding activity that maintains unfolded intermediates on-pathway to their functional folded states (65-67). To further demonstrate how tau-mediated sequestration of chaperones affects proteostasis in the cytoplasm, we examined the protein folding arm of the PN using a folding sensor that had been developed using firefly luciferase whose folding *in vivo* was known to be dependent upon HSC70 and HSP90 (67,68). We therefore employed the metastable protein folding sensor EGFP-firefly luciferase DM (fLucDM-EGFP) mutant (69) delivered by lentivirus that was conditionally expressed with tau P301S protein (Fig. S4). Whereas the EGFP protein (Fig. 4A a-d) does not colocalize with PG5/MC1 tau inclusions (Fig. 4A c, arrows; 4B i-j), the fLucDM-EGFP folding sensor (Fig. 4A e-h) colocalized with PG5/MC1 positive inclusions (Fig. 4A g, arrows; 4B k-l). In contrast, sequestration or aggregation of the fLucDM-EGFP folding sensor in MC1 positive cells was not observed (Fig. 4A g, arrowheads). The colocalization between PG5 tau inclusions and fLucDM-EGFP gave a PCC value of 0.61 indicating strong level of interaction (Fig. 4B k-l, quantified in 4C) relative to the PCC value of -0.32 for PG5 positive tau inclusions and EGFP protein (Fig. 4B i-j and 4C). MC1 positive tau species also showed poor correlation with the folding sensor (PCC value of 0.06). These results suggest that changes in tau conformation detected by MC1 and inhibition of CME precedes the inhibitory effects of tau aggregates (PG5/MC1 positive) on protein folding.

**Enhancing chaperone levels reverses the tau inhibitory effects on clathrin-mediated endocytosis**

If the sequestration of cytoplasmic chaperones by tau aggregates interferes with chaperone dependent cellular activities, this would suggest that these cellular activities could be restored by enhancing the levels of these chaperones. We therefore examined the effects of small molecule proteostasis regulators that activate HSF1 and consequently the expression of cytosolic chaperones (70). Three small molecules (A3, C1 and F1) previously shown to activate HSF1 (70) and the expression of HSC70/HSP70 in HEK293 tau P301S cells by 2-3-fold (Fig. S5 a-d, quantified in e) were employed. Using a protocol in which tau P301S cells were seeded to induce tau aggregation for two days followed by addition of either A3, C1 or F1 for 24 hours, we examined three cell populations (negative, PG5/MC1 positive and MC1 positive only) (Fig. 5 e-p) for transferrin uptake relative to vehicle alone treated cells (Fig. 5 a-d). All three proteostasis regulators either partially or completely restored CME in the PG5/MC1 cells and MC1 cells (Fig. 5 g, k and o, arrows and arrowheads, compared to panel c, quantified in 5q). It was notable that while CME was restored, the level of tau aggregates was not notably affected as measured by the number of PG5/MC1 positive cells (Fig. S5f, 24 hours).

However, by extending the treatment period of F1 to 48 hours, we observed a 54% reduction in tau aggregate containing cells (Fig. S5f, 48 hours). These results indicate that enhancing the levels of chaperones in this protocol can prevent the decline in chaperone dependent activities and thus alleviate cellular toxicity from tau aggregation.

As a complement to small molecule proteostasis regulators, we employed a conditional genetic switch to increase the levels of HSC70. HEK293 tau P301S cells stably expressing V5-HSC70 under the control of the cumate conditional promoter were established (Fig. 6 A and B) for the conditional expression of V5-tagged HSC70 (Fig. 6A, b vs. d, anti-V5 antibody) (Fig. 6B, f vs. h, anti-HSC70/HSP70 antibody). Tetracycline induced tau P301S expressing cells were seeded to induce tau aggregation and cumate was added at day 2 post seeding to induce HSC70 expression for 24 hours. Transferrin uptake was quantified in cells with and without tau aggregation (Fig. 6C). Cumate-induced expression of HSC70 alone does not affect transferrin uptake in control cells but restores transferrin uptake to unaffected levels in MC1 only cells and partially in PG5/MC1 positive cells (32.4% compared to 55.8% inhibition with or without V5-HSC70 expression).

To further support the deleterious consequences of chaperone competition, we performed experiments in which chaperone levels were reduced to determine whether tau aggregation and the inhibition of CME was exacerbated. This was accomplished by expression of siRNA to the HSC70 (HSPA8) in HEK293 tau P301S cells for 48 hours after which the cytosolic level of HSC70 was reduced by 3.6 fold (Fig. S6A, compare a to c; quantified in e). siRNA treatment was conducted 24 hours after the cells were seeded with tau seeds at a 1:10 ratio. The results showed that control siRNA transfected cells were 7% MC1-only positive and 11% PG5/MC1 positive, whereas cells treated with HSPA8 siRNA showed a significant reduction of MC1-only cells to 0.3% and increased number (23%) of PG5 positive cells (Fig. S6A, f). This further supports the importance of HSC70 in the transition between the MC1 and PG5 conformations of tau. Following HSC70 genetic knockdown, transferrin uptake in cells without tau inclusions was reduced by 28% indicating the sensitivity of CME to cellular HSC70 (Fig. S6B, o) (23). CME in PG5 positive cells was further reduced compared to the control siRNA treated cells (39% vs. 53% reduction) (Figure S6B, i vs. m, arrows, quantified in o).

**Small molecule proteostasis regulators reduce the sequestration of luciferase folding sensor by tau inclusions**

To further demonstrate that reduction in the cytoplasmic pool of chaperones by sequestration in inclusions can be overcome by increasing the levels of cytoplasmic chaperones, we examined whether small molecule proteostasis regulators that activate HSF1 and expression of cytoplasmic chaperones can rescue the misfolding and subsequent sequestration of luciferase by tau inclusions. HEK293 tau P301S cells expressing the fLucDM-EGFP sensor were treated with compound A3 for 24 hours after seeding, and the levels of luciferase colocalization with the PG5 tau inclusions were then measured. In DMSO treated cells, fLucDM-EGFP showed strong colocalization with PG5 tau inclusions with an average PCC of 0.63 (Figure 7 a-e, arrows, quantified in k) that was reduced to PPC of 0.29 in cells treated with A3 (Figure

7 h-j, arrows, quantified in k). Likewise, the colocalization between MC1 tau and luciferase was 0.28 in DMSO treated cells that reduced to PCC of 0.18 in A3 treated cells.

These studies reveal that chaperone competition by tau aggregation has selective inhibitory effects on vesicular trafficking and the protein folding arms of proteostasis that can be reversed, and moreover, that different classes of protein conformation states can interfere with certain arms of the PN.

## Discussion

Tau aggregation has profound consequences on diverse cellular events (31,71), and here we demonstrate that tau dependent sequestration of cytoplasmic molecular chaperones leads to chaperone mislocalization and the functional inhibition of chaperone dependent events of protein folding and clathrin-mediated endocytosis. While tau inhibitory effects on protein folding will undoubtedly have broad negative consequences on protein function and cellular health, the loss of CME is particularly relevant for neuronal signaling and receptor activity regulated by ligand-stimulated internalization through clathrin-coated vesicles (72-74). Failure in endocytic internalization is associated with the abnormal accumulation of activated receptors at the cell surface affecting downstream signaling events such as memory consolidation and long-term depression (75-77). Moreover, persistent signaling from glutamate receptors at the plasma membrane results in excitotoxicity and eventual neuronal cell death (78,79), and CME is essential for the retrieval of synaptic vesicles after neurotransmitter release (80-83).

Among the many client interactions for HSC70, interaction with tau directs productive folding and prevents aggregation (44). Upon dissociation of tau from microtubules, HSC70 re-engages with tau to facilitate folding into a conformation recognized by the MC1 antibody. While this serves as a protective mechanism for wild type tau, this interaction may also promote protein aggregation when mutant tau persists in a more unstructured state (49). Our data shows that the appearance of the MC1 conformational state of tau is associated with CME failure that is detected before the appearance of PG5 positive tau inclusions and the stable sequestration of HSC70. The timing of these cellular events suggests that the inhibition of CME is an early cellular event of Tauopathy and precedes failure of other cellular processes such as chaperone-dependent protein folding. This is consistent with observations that tau oligomers corresponding to the MC1 tau conformational species initiate cellular toxicity. Because the MC1 conformational states of tau corresponds to the transition of chaperone sequestration, we suggest that chaperone-dependent cellular processes are not equally sensitive to aggregation induced failure and that CME, in particular, is more at risk by comparison with protein folding.

Inhibition of the protein folding arm of the PN by tau aggregation would further exacerbate the consequence of tau aggregation and accelerate misfolding and aggregation of other structurally challenged proteins with missense mutations, errors and structural instabilities (15,84,85). We posit that these events, initiated by tau aggregation, would lead to a vicious cycle of self-propagated protein damage that contribute to proteostasis

collapse. Our data further shows that tau inclusions associate with a number of cytoplasmic molecular chaperones, which over time would be predicted to interfere with a multitude of cellular processes. Although in this study we have only focused on two specific HSC70 dependent cellular activities of protein folding and CME, our results suggest a much broader negative consequence of global chaperone sequestration.

A basis for proteostasis collapse with implications for aging and protein conformational disease has been observed in *C. elegans* whereby the regulation of the heat shock response in adult animals is repressed at reproductive maturity by affecting chromatin structure and HSF1 binding at genes encoding molecular chaperones (86). The programmed decline of the heat shock response and stress induced expression of molecular chaperones suggests that maintaining and enhancing chaperone expression and function in aging could have beneficial consequences on proteome health. Here, we show that the decline of the chaperone-regulated arms of the PN in tau expressing cells could be compensated by small molecule proteostasis regulators that enhanced expression of cytoplasmic chaperones and by a genetic approach using conditional expression of HSC70. Moreover, these experiments suggest that restoration of clathrin-mediated endocytosis and therefore recycling of receptors important to neuronal signaling could prevent neuronal dysfunction in tau-associated diseases.

## Materials and Methods

### DNA plasmids and antibodies

To generate the lentiviral expression plasmid encoding the firefly luciferase folding sensor, the blunt end fragment was released from pCIneoFlucDM-EGFP (69) following Eco53KI and PuvII digestion and ligated to pENTR11-Dual selection vector (Invitrogen) that was linearized by XmnI and EcoRV. Gateway LR reaction was performed to translocate the fLucDM-EGFP encoding fragment into the pLenti CMV/TO Puro DEST (670-1) vector (Addgene 17293) (87). The open reading frame of human HSC70 with a V5 tag at the N-terminus was PCR amplified using pcDNA5/FRT/TO V5 HSPA8 (Addgene 19514) (88) and the PCR fragment was cloned into the SparQ All-in-one Cumate Switch Inducible Lentivector (System Biosciences, QM800A-1) using the NheI and BstBI restriction sites.

The rabbit polyclonal antibody recognizing HSC70 as well as stress-inducible HSP70 used for immunofluorescence was from Santa Cruz Biotechnology (H300, sc-33575, IF 1:300). Commercial antibodies recognizing the following were used: anti-V5 (rabbit IgG, V8137, Sigma, IF 1:2000), anti-HSP110 (rabbit polyclonal, SPC-195, StressMarq Biosciences Inc., IF 1:500), anti-DNAJB1 (rabbit polyclonal, ADI-SPA-400, Enzo Life Sciences, IF 1:500), anti-HSP90α (rabbit polyclonal, ADI-SPS-771, Enzo Life Sciences, IF 1:500), anti-HSP90β (rabbit polyclonal, ADI-SPA-844, Enzo Life Sciences, IF 1:500), DyLight™ 488 conjugated HSC70 (mouse monoclonal,1B5, ADI-SPA-815-488-E, Enzo Life Sciences, IF 1:500), anti-HSP70 (mouse monoclonal IgG1, 4G4, IF 1:500), anti-HSP27 (rabbit polyclonal, #2442, Cell Signaling, IF 1:500), anti-total tau HT7 (mouse monoclonal IgG1, MN1000, Thermo Fisher Scientific, IF 1:500) and various Alexa Fluor-conjugated secondary antibodies (Thermo Fisher Scientific). The following tau antibodies were kind gifts

from Dr. Peter Davies (Albert Einstein College of Medicine, New York): total tau CP27 (mouse monoclonal IgG2a, IF 1:2000) and pathological tau specific antibodies including MC1 (mouse monoclonal IgG1, IF 1:8500) or PG5 (mouse monoclonal IgG3, IF 1:3000).

**Tau seeding and aggregation assay and transferrin assay**

Mock Flp-In™ 293 T-REx cells and T-REx™ HEK293 derived tau 1N4R WT and tau 1N4R P301S cells (57) were maintained at 37 $^{o}$C and 5% $CO_2$ in DMEM complete medium supplemented with 10% heat-inactivated FBS (Gibco, 16140071) together with 1% Penicillin/Streptomycin/Glutamine. Cells were plated at 5 × $10^5$ cells/well in 12-well plates and induced with 1 µg/ml tetracycline for 24 hours to express exogenous tau protein. Cells were then incubated with sarkosyl-insoluble tau P301S seeds (57,89) at 1:40 dilution in OPTI-MEM for 3 hours. After removing seeds, cells were incubated in complete medium containing tetracycline for an additional 24 hours. Cells were transferred to tetracycline free medium for another 48 hours before fixation and immunostaining to detect pathological tau conformation.

For the transferrin assay, 48 hours after treatment with insoluble tau seeds cells were replated at 3 x $10^5$ cells/well onto fibronectin-coated coverslips in a 12-well plate. Transferrin internalization was performed 24 hours post replating. Cells were placed in pre-warmed serum-free DMEM for 60 min and then incubated with Alexa 555-conjugated transferrin at 16.7 µg/ml (Life Technologies) in pre-warmed DMEM-0.1% BSA for 15 min. The plates were placed on ice, cells washed with ice cold PBS after removing media. Cells were acid-washed by a 5-min incubation with ice-cold acid wash buffer (0.1 M glycine, pH 2.5, 150 mM NaCl) to remove surface-bound transferrin. Cells were then fixed with 4% paraformaldehyde in PBS for 20 min and immunostained with antibodies recognizing total tau (HT7) and pathological tau species (PG5 and MC1).

**Establishing stable expression cell lines using lentivirus**

T-REx™ HEK293 tau 1N4R P301S cells were infected with lentivirus encoding luciferase folding sensor fLucDM-EGFP or V5-HSPA8 for inducible protein expression. Three days after infection, cells were transferred to medium containing 2 µg/ml puromycin and maintained until puromycin selection was complete. Stable single clones for the proteostasis reporter lines were further selected by dilution cloning. The resulting reporter cell lines were maintained in complete DMEM medium supplemented with 200 µg/ml Zeocin™, 5 µg/ml blasticidin and 2 µg/ml puromycin.

**Small molecule regulators of PN treatment**

HEK293 tau P301S cells were induced to express tau P301S protein and HEK293 tau P301S-fLucDM-EGFP cells were induced to express both tau P301S and fLucDM-EGFP protein for 24 hours. Cells were seeded with sarkosyl-insoluble tau seeds. One day post tau seeding, cells were replated at 2 x $10^5$ cells/well in a 12-well plate on fibronectin-coated coverslips and grown for an additional 24 hours. Small molecule PN regulators at the indicated concentrations premixed with fresh complete medium were added to cells which were then incubate for 24 hours. Cells were then fixed and immunostained to test the induction of HSC70/HSP70 protein expression. Transferrin uptake assay was performed as described.

**Tunable expression of human HSC70 protein**

The HEK293 tau P301S stable cell line encoding V5 tagged-HSC70 protein

under the control of the cumate-inducible promoter was generated. Seeding and aggregation assay was performed as described. Two days post seeding, 300 µg/ml cumate (System Biosciences, QM150A-1) was added to the cells that were then incubated for an additional 24 hours to induce V5 tagged human HSC70 expression. Transferrin uptake was performed. Cells were also immunostained with anti-V5 and -HSC70/HSP70 antibodies.

**Indirect immunofluorescence, microscopy and image analysis**

Cells were fixed with 4% paraformaldehyde in PBS for 20 min. Cells were permeabilized in PBS containing 0.2% Triton X-100 and 1% BSA for 10 min. Cells were blocked with Odyssey® Blocking Buffer (LI-COR Biosciences, 927-40000) for 1 hour and sequentially incubated with primary antibodies and Alexa Fluor® conjugated secondary antibodies in Odyssey® Blocking Buffer for 1 hour at room temperature with PBS washes after each antibody treatment. Coverslips were mounted using Fluoromount-G (Southern Biotech).

Image acquisition was conducted as described (23). Figure S2, S6 and 7 were captured with a Leica TCS SP8 confocal microscope and all other images were obtained using a Leica SP5 II laser scanning confocal microscope. For image presentation, maximal projections of the z-series were created and brightness was adjusted across the entire image using LAS AF lite software. Images shown are representative of three independent experiments.

For quantification of transferrin internalization or endogenous chaperone expression levels, raw 16-bit z-series were converted to sum slice projections using ImageJ. Individual cells were outlined as regions of interest (ROI) and the total integrated fluorescence intensities were measured. The mean intensities of three ROIs outside of the cell were also measured to serve as background intensity. The corrected total cell fluorescence (CTCF) was calculated using the following formula:

CTCF = Integrated Density of selected cell – (Area of selected cell X Mean fluorescence of background readings).

CTCF of individual cell population was plotted using GraphPad Prism software with 1 x $10^3$ fluorescence unit per cell. For transferrin analysis, it was empirically determined that the cells with the 5% highest and lowest fluorescence intensities reliably represented mechanically broken or dead cells, respectively, and these were excluded from the analyses (23).

For colocalization analysis, Pearson correlation coefficient (PCC) were calculated from regions of interests identified from confocal image stacks using the Fiji ImageJ colocalization plugin Coloc 2 with a calculated point spread function at 3 and 10 Costes shuffling Iterations.

**Acknowledgements**

We thank Sara Fernandez Dunne from the Northwestern High Throughput Analysis Laboratory and Jessica Elizabeth Hornick from the Northwestern Biological Imaging Facility for their support of instrumental usage and data analysis. This work was supported by National Institutes of Health (National Institute on Aging), the Daniel F. and Ada L. Rice Foundation to RIM and a research grant from Eli Lilly & Co Ltd, Lilly Research Centre.

The authors declare that they have no conflicts of interest with the contents of this article.

## References:


1. Knowles, T. P., Vendruscolo, M., and Dobson, C. M. (2014) The amyloid state and its association with protein misfolding diseases. *Nature reviews. Molecular cell biology* **15**, 384-396
2. Chiti, F., and Dobson, C. M. (2006) Protein misfolding, functional amyloid, and human disease. *Annual review of biochemistry* **75**, 333-366
3. Soto, C. (2003) Unfolding the role of protein misfolding in neurodegenerative diseases. *Nature reviews. Neuroscience* **4**, 49-60
4. Bucciantini, M., Giannoni, E., Chiti, F., Baroni, F., Formigli, L., Zurdo, J., Taddei, N., Ramponi, G., Dobson, C. M., and Stefani, M. (2002) Inherent toxicity of aggregates implies a common mechanism for protein misfolding diseases. *Nature* **416**, 507-511
5. Balch, W. E., Morimoto, R. I., Dillin, A., and Kelly, J. W. (2008) Adapting proteostasis for disease intervention. *Science* **319**, 916-919
6. Wolff, S., Weissman, J. S., and Dillin, A. (2014) Differential scales of protein quality control. *Cell* **157**, 52-64
7. Klaips, C. L., Jayaraj, G. G., and Hartl, F. U. (2018) Pathways of cellular proteostasis in aging and disease. *The Journal of cell biology* **217**, 51-63
8. Labbadia, J., and Morimoto, R. I. (2015) The biology of proteostasis in aging and disease. *Annual review of biochemistry* **84**, 435-464
9. Gidalevitz, T., Kikis, E. A., and Morimoto, R. I. (2010) A cellular perspective on conformational disease: the role of genetic background and proteostasis networks. *Current opinion in structural biology* **20**, 23-32
10. Bence, N. F., Sampat, R. M., and Kopito, R. R. (2001) Impairment of the ubiquitin-proteasome system by protein aggregation. *Science* **292**, 1552-1555
11. Woerner, A. C., Frottin, F., Hornburg, D., Feng, L. R., Meissner, F., Patra, M., Tatzelt, J., Mann, M., Winklhofer, K. F., Hartl, F. U., and Hipp, M. S. (2016) Cytoplasmic protein aggregates interfere with nucleocytoplasmic transport of protein and RNA. *Science* **351**, 173-176
12. Satyal, S. H., Schmidt, E., Kitagawa, K., Sondheimer, N., Lindquist, S., Kramer, J. M., and Morimoto, R. I. (2000) Polyglutamine aggregates alter protein folding homeostasis in Caenorhabditis elegans. *Proceedings of the National Academy of Sciences of the United States of America* **97**, 5750-5755
13. Holmberg, C. I., Staniszewski, K. E., Mensah, K. N., Matouschek, A., and Morimoto, R. I. (2004) Inefficient degradation of truncated polyglutamine proteins by the proteasome. *The EMBO journal* **23**, 4307-4318
14. Bennett, E. J., Bence, N. F., Jayakumar, R., and Kopito, R. R. (2005) Global impairment of the ubiquitin-proteasome system by nuclear or cytoplasmic protein aggregates precedes inclusion body formation. *Molecular cell* **17**, 351-365
15. Gidalevitz, T., Ben-Zvi, A., Ho, K. H., Brignull, H. R., and Morimoto, R. I. (2006) Progressive disruption of cellular protein folding in models of polyglutamine diseases. *Science* **311**, 1471-1474
16. Stenoien, D. L., Cummings, C. J., Adams, H. P., Mancini, M. G., Patel, K., DeMartino, G. N., Marcelli, M., Weigel, N. L., and Mancini, M. A. (1999) Polyglutamine-expanded androgen receptors form aggregates that sequester heat shock proteins, proteasome components and SRC-1, and are suppressed by the HDJ-2 chaperone. *Human molecular genetics* **8**, 731-741
17. Olzscha, H., Schermann, S. M., Woerner, A. C., Pinkert, S., Hecht, M. H., Tartaglia, G. G., Vendruscolo, M., Hayer-Hartl, M., Hartl, F. U., and Vabulas, R. M. (2011) Amyloid-

like aggregates sequester numerous metastable proteins with essential cellular functions. *Cell* **144**, 67-78
18. Escusa-Toret, S., Vonk, W. I., and Frydman, J. (2013) Spatial sequestration of misfolded proteins by a dynamic chaperone pathway enhances cellular fitness during stress. *Nature cell biology* **15**, 1231-1243
19. Park, S. H., Kukushkin, Y., Gupta, R., Chen, T., Konagai, A., Hipp, M. S., Hayer-Hartl, M., and Hartl, F. U. (2013) PolyQ proteins interfere with nuclear degradation of cytosolic proteins by sequestering the Sis1p chaperone. *Cell* **154**, 134-145
20. Schmidt, T., Lindenberg, K. S., Krebs, A., Schols, L., Laccone, F., Herms, J., Rechsteiner, M., Riess, O., and Landwehrmeyer, G. B. (2002) Protein surveillance machinery in brains with spinocerebellar ataxia type 3: redistribution and differential recruitment of 26S proteasome subunits and chaperones to neuronal intranuclear inclusions. *Annals of neurology* **51**, 302-310
21. Chai, Y., Shao, J., Miller, V. M., Williams, A., and Paulson, H. L. (2002) Live-cell imaging reveals divergent intracellular dynamics of polyglutamine disease proteins and supports a sequestration model of pathogenesis. *Proceedings of the National Academy of Sciences of the United States of America* **99**, 9310-9315
22. Donaldson, K. M., Li, W., Ching, K. A., Batalov, S., Tsai, C. C., and Joazeiro, C. A. (2003) Ubiquitin-mediated sequestration of normal cellular proteins into polyglutamine aggregates. *Proceedings of the National Academy of Sciences of the United States of America* **100**, 8892-8897
23. Yu, A., Shibata, Y., Shah, B., Calamini, B., Lo, D. C., and Morimoto, R. I. (2014) Protein aggregation can inhibit clathrin-mediated endocytosis by chaperone competition. *Proceedings of the National Academy of Sciences of the United States of America* **111**, E1481-1490
24. Witman, G. B., Cleveland, D. W., Weingarten, M. D., and Kirschner, M. W. (1976) Tubulin requires tau for growth onto microtubule initiating sites. *Proceedings of the National Academy of Sciences of the United States of America* **73**, 4070-4074
25. Grundke-Iqbal, I., Iqbal, K., Tung, Y. C., Quinlan, M., Wisniewski, H. M., and Binder, L. I. (1986) Abnormal phosphorylation of the microtubule-associated protein tau (tau) in Alzheimer cytoskeletal pathology. *Proceedings of the National Academy of Sciences of the United States of America* **83**, 4913-4917
26. Hong, M., Zhukareva, V., Vogelsberg-Ragaglia, V., Wszolek, Z., Reed, L., Miller, B. I., Geschwind, D. H., Bird, T. D., McKeel, D., Goate, A., Morris, J. C., Wilhelmsen, K. C., Schellenberg, G. D., Trojanowski, J. Q., and Lee, V. M. (1998) Mutation-specific functional impairments in distinct tau isoforms of hereditary FTDP-17. *Science* **282**, 1914-1917
27. Nacharaju, P., Lewis, J., Easson, C., Yen, S., Hackett, J., Hutton, M., and Yen, S. H. (1999) Accelerated filament formation from tau protein with specific FTDP-17 missense mutations. *FEBS letters* **447**, 195-199
28. Barghorn, S., Zheng-Fischhofer, Q., Ackmann, M., Biernat, J., von Bergen, M., Mandelkow, E. M., and Mandelkow, E. (2000) Structure, microtubule interactions, and paired helical filament aggregation by tau mutants of frontotemporal dementias. *Biochemistry* **39**, 11714-11721
29. Schweers, O., Schonbrunn-Hanebeck, E., Marx, A., and Mandelkow, E. (1994) Structural studies of tau protein and Alzheimer paired helical filaments show no evidence for beta-structure. *The Journal of biological chemistry* **269**, 24290-24297
30. Lee, V. M., Goedert, M., and Trojanowski, J. Q. (2001) Neurodegenerative tauopathies. *Annual review of neuroscience* **24**, 1121-1159
31. Wang, Y., and Mandelkow, E. (2016) Tau in physiology and pathology. *Nature reviews. Neuroscience* **17**, 22-35

32. Spillantini, M. G., and Goedert, M. (2013) Tau pathology and neurodegeneration. *The Lancet. Neurology* **12**, 609-622
33. Kopke, E., Tung, Y. C., Shaikh, S., Alonso, A. C., Iqbal, K., and Grundke-Iqbal, I. (1993) Microtubule-associated protein tau. Abnormal phosphorylation of a non-paired helical filament pool in Alzheimer disease. *The Journal of biological chemistry* **268**, 24374-24384
34. Frost, B., Jacks, R. L., and Diamond, M. I. (2009) Propagation of tau misfolding from the outside to the inside of a cell. *The Journal of biological chemistry* **284**, 12845-12852
35. Guo, J. L., and Lee, V. M. (2011) Seeding of normal Tau by pathological Tau conformers drives pathogenesis of Alzheimer-like tangles. *The Journal of biological chemistry* **286**, 15317-15331
36. Clavaguera, F., Bolmont, T., Crowther, R. A., Abramowski, D., Frank, S., Probst, A., Fraser, G., Stalder, A. K., Beibel, M., Staufenbiel, M., Jucker, M., Goedert, M., and Tolnay, M. (2009) Transmission and spreading of tauopathy in transgenic mouse brain. *Nature cell biology* **11**, 909-913
37. de Calignon, A., Polydoro, M., Suarez-Calvet, M., William, C., Adamowicz, D. H., Kopeikina, K. J., Pitstick, R., Sahara, N., Ashe, K. H., Carlson, G. A., Spires-Jones, T. L., and Hyman, B. T. (2012) Propagation of tau pathology in a model of early Alzheimer's disease. *Neuron* **73**, 685-697
38. Ahmed, Z., Cooper, J., Murray, T. K., Garn, K., McNaughton, E., Clarke, H., Parhizkar, S., Ward, M. A., Cavallini, A., Jackson, S., Bose, S., Clavaguera, F., Tolnay, M., Lavenir, I., Goedert, M. et al. (2014) A novel in vivo model of tau propagation with rapid and progressive neurofibrillary tangle pathology: the pattern of spread is determined by connectivity, not proximity. *Acta neuropathologica* **127**, 667-683
39. Iba, M., McBride, J. D., Guo, J. L., Zhang, B., Trojanowski, J. Q., and Lee, V. M. (2015) Tau pathology spread in PS19 tau transgenic mice following locus coeruleus (LC) injections of synthetic tau fibrils is determined by the LC's afferent and efferent connections. *Acta neuropathologica* **130**, 349-362
40. Kaufman, S. K., Sanders, D. W., Thomas, T. L., Ruchinskas, A. J., Vaquer-Alicea, J., Sharma, A. M., Miller, T. M., and Diamond, M. I. (2016) Tau Prion Strains Dictate Patterns of Cell Pathology, Progression Rate, and Regional Vulnerability In Vivo. *Neuron* **92**, 796-812
41. Sanders, D. W., Kaufman, S. K., DeVos, S. L., Sharma, A. M., Mirbaha, H., Li, A., Barker, S. J., Foley, A. C., Thorpe, J. R., Serpell, L. C., Miller, T. M., Grinberg, L. T., Seeley, W. W., and Diamond, M. I. (2014) Distinct tau prion strains propagate in cells and mice and define different tauopathies. *Neuron* **82**, 1271-1288
42. Wu, J. W., Hussaini, S. A., Bastille, I. M., Rodriguez, G. A., Mrejeru, A., Rilett, K., Sanders, D. W., Cook, C., Fu, H., Boonen, R. A., Herman, M., Nahmani, E., Emrani, S., Figueroa, Y. H., Diamond, M. I. et al. (2016) Neuronal activity enhances tau propagation and tau pathology in vivo. *Nature neuroscience* **19**, 1085-1092
43. DeVos, S. L., Corjuc, B. T., Oakley, D. H., Nobuhara, C. K., Bannon, R. N., Chase, A., Commins, C., Gonzalez, J. A., Dooley, P. M., Frosch, M. P., and Hyman, B. T. (2018) Synaptic Tau Seeding Precedes Tau Pathology in Human Alzheimer's Disease Brain. *Frontiers in neuroscience* **12**, 267
44. Dou, F., Netzer, W. J., Tanemura, K., Li, F., Hartl, F. U., Takashima, A., Gouras, G. K., Greengard, P., and Xu, H. (2003) Chaperones increase association of tau protein with microtubules. *Proceedings of the National Academy of Sciences of the United States of America* **100**, 721-726
45. Petrucelli, L., Dickson, D., Kehoe, K., Taylor, J., Snyder, H., Grover, A., De Lucia, M., McGowan, E., Lewis, J., Prihar, G., Kim, J., Dillmann, W. H., Browne, S. E., Hall, A.,

Voellmy, R. et al. (2004) CHIP and Hsp70 regulate tau ubiquitination, degradation and aggregation. *Human molecular genetics* **13**, 703-714
46. Dickey, C. A., Kamal, A., Lundgren, K., Klosak, N., Bailey, R. M., Dunmore, J., Ash, P., Shoraka, S., Zlatkovic, J., Eckman, C. B., Patterson, C., Dickson, D. W., Nahman, N. S., Jr., Hutton, M., Burrows, F. et al. (2007) The high-affinity HSP90-CHIP complex recognizes and selectively degrades phosphorylated tau client proteins. *The Journal of clinical investigation* **117**, 648-658
47. Eroglu, B., Moskophidis, D., and Mivechi, N. F. (2010) Loss of Hsp110 leads to age-dependent tau hyperphosphorylation and early accumulation of insoluble amyloid beta. *Molecular and cellular biology* **30**, 4626-4643
48. Jinwal, U. K., Koren, J., 3rd, Borysov, S. I., Schmid, A. B., Abisambra, J. F., Blair, L. J., Johnson, A. G., Jones, J. R., Shults, C. L., O'Leary, J. C., 3rd, Jin, Y., Buchner, J., Cox, M. B., and Dickey, C. A. (2010) The Hsp90 cochaperone, FKBP51, increases Tau stability and polymerizes microtubules. *The Journal of neuroscience : the official journal of the Society for Neuroscience* **30**, 591-599
49. Jinwal, U. K., O'Leary, J. C., 3rd, Borysov, S. I., Jones, J. R., Li, Q., Koren, J., 3rd, Abisambra, J. F., Vestal, G. D., Lawson, L. Y., Johnson, A. G., Blair, L. J., Jin, Y., Miyata, Y., Gestwicki, J. E., and Dickey, C. A. (2010) Hsc70 rapidly engages tau after microtubule destabilization. *The Journal of biological chemistry* **285**, 16798-16805
50. Mok, S. A., Condello, C., Freilich, R., Gillies, A., Arhar, T., Oroz, J., Kadavath, H., Julien, O., Assimon, V. A., Rauch, J. N., Dunyak, B. M., Lee, J., Tsai, F. T. F., Wilson, M. R., Zweckstetter, M. et al. (2018) Mapping interactions with the chaperone network reveals factors that protect against tau aggregation. *Nature structural & molecular biology* **25**, 384-393
51. Abisambra, J. F., Blair, L. J., Hill, S. E., Jones, J. R., Kraft, C., Rogers, J., Koren, J., 3rd, Jinwal, U. K., Lawson, L., Johnson, A. G., Wilcock, D., O'Leary, J. C., Jansen-West, K., Muschol, M., Golde, T. E. et al. (2010) Phosphorylation dynamics regulate Hsp27-mediated rescue of neuronal plasticity deficits in tau transgenic mice. *The Journal of neuroscience : the official journal of the Society for Neuroscience* **30**, 15374-15382
52. Baughman, H. E. R., Clouser, A. F., Klevit, R. E., and Nath, A. (2018) HspB1 and Hsc70 chaperones engage distinct tau species and have different inhibitory effects on amyloid formation. *The Journal of biological chemistry*
53. Voss, K., Combs, B., Patterson, K. R., Binder, L. I., and Gamblin, T. C. (2012) Hsp70 alters tau function and aggregation in an isoform specific manner. *Biochemistry* **51**, 888-898
54. Karagoz, G. E., Duarte, A. M., Akoury, E., Ippel, H., Biernat, J., Moran Luengo, T., Radli, M., Didenko, T., Nordhues, B. A., Veprintsev, D. B., Dickey, C. A., Mandelkow, E., Zweckstetter, M., Boelens, R., Madl, T. et al. (2014) Hsp90-Tau complex reveals molecular basis for specificity in chaperone action. *Cell* **156**, 963-974
55. Wang, Q., Woltjer, R. L., Cimino, P. J., Pan, C., Montine, K. S., Zhang, J., and Montine, T. J. (2005) Proteomic analysis of neurofibrillary tangles in Alzheimer disease identifies GAPDH as a detergent-insoluble paired helical filament tau binding protein. *FASEB journal : official publication of the Federation of American Societies for Experimental Biology* **19**, 869-871
56. Minjarez, B., Valero Rustarazo, M. L., Sanchez del Pino, M. M., Gonzalez-Robles, A., Sosa-Melgarejo, J. A., Luna-Munoz, J., Mena, R., and Luna-Arias, J. P. (2013) Identification of polypeptides in neurofibrillary tangles and total homogenates of brains with Alzheimer's disease by tandem mass spectrometry. *Journal of Alzheimer's disease : JAD* **34**, 239-262
57. Falcon, B., Cavallini, A., Angers, R., Glover, S., Murray, T. K., Barnham, L., Jackson, S., O'Neill, M. J., Isaacs, A. M., Hutton, M. L., Szekeres, P. G., Goedert, M., and Bose, S.

(2015) Conformation determines the seeding potencies of native and recombinant tau aggregates. *The Journal of biological chemistry* **290**, 1049-1065
58. Wolozin, B. L., Pruchnicki, A., Dickson, D. W., and Davies, P. (1986) A neuronal antigen in the brains of Alzheimer patients. *Science* **232**, 648-650
59. Jicha, G. A., Bowser, R., Kazam, I. G., and Davies, P. (1997) Alz-50 and MC-1, a new monoclonal antibody raised to paired helical filaments, recognize conformational epitopes on recombinant tau. *Journal of neuroscience research* **48**, 128-132
60. Weaver, C. L., Espinoza, M., Kress, Y., and Davies, P. (2000) Conformational change as one of the earliest alterations of tau in Alzheimer's disease. *Neurobiology of aging* **21**, 719-727
61. Vingtdeux, V., Davies, P., Dickson, D. W., and Marambaud, P. (2011) AMPK is abnormally activated in tangle- and pre-tangle-bearing neurons in Alzheimer's disease and other tauopathies. *Acta neuropathologica* **121**, 337-349
62. Jicha, G. A., Weaver, C., Lane, E., Vianna, C., Kress, Y., Rockwood, J., and Davies, P. (1999) cAMP-dependent protein kinase phosphorylations on tau in Alzheimer's disease. *The Journal of neuroscience : the official journal of the Society for Neuroscience* **19**, 7486-7494
63. Vitale, F., Giliberto, L., Ruiz, S., Steslow, K., Marambaud, P., and d'Abramo, C. (2018) Anti-tau conformational scFv MC1 antibody efficiently reduces pathological tau species in adult JNPL3 mice. *Acta neuropathologica communications* **6**, 82
64. Mead, E., Kestoras, D., Gibson, Y., Hamilton, L., Goodson, R., Jones, S., Eversden, S., Davies, P., O'Neill, M., Hutton, M., Szekeres, P., and Wolak, J. (2016) Halting of Caspase Activity Protects Tau from MC1-Conformational Change and Aggregation. *Journal of Alzheimer's disease : JAD* **54**, 1521-1538
65. Parsell, D. A., Kowal, A. S., Singer, M. A., and Lindquist, S. (1994) Protein disaggregation mediated by heat-shock protein Hsp104. *Nature* **372**, 475-478
66. Freeman, B. C., and Morimoto, R. I. (1996) The human cytosolic molecular chaperones hsp90, hsp70 (hsc70) and hdj-1 have distinct roles in recognition of a non-native protein and protein refolding. *The EMBO journal* **15**, 2969-2979
67. Frydman, J., Nimmesgern, E., Ohtsuka, K., and Hartl, F. U. (1994) Folding of nascent polypeptide chains in a high molecular mass assembly with molecular chaperones. *Nature* **370**, 111-117
68. Freeman, B. C., Myers, M. P., Schumacher, R., and Morimoto, R. I. (1995) Identification of a regulatory motif in Hsp70 that affects ATPase activity, substrate binding and interaction with HDJ-1. *The EMBO journal* **14**, 2281-2292
69. Gupta, R., Kasturi, P., Bracher, A., Loew, C., Zheng, M., Villella, A., Garza, D., Hartl, F. U., and Raychaudhuri, S. (2011) Firefly luciferase mutants as sensors of proteome stress. *Nature methods* **8**, 879-884
70. Calamini, B., Silva, M. C., Madoux, F., Hutt, D. M., Khanna, S., Chalfant, M. A., Saldanha, S. A., Hodder, P., Tait, B. D., Garza, D., Balch, W. E., and Morimoto, R. I. (2012) Small-molecule proteostasis regulators for protein conformational diseases. *Nature chemical biology* **8**, 185-196
71. Spires-Jones, T. L., Stoothoff, W. H., de Calignon, A., Jones, P. B., and Hyman, B. T. (2009) Tau pathophysiology in neurodegeneration: a tangled issue. *Trends in neurosciences* **32**, 150-159
72. McMahon, H. T., and Boucrot, E. (2011) Molecular mechanism and physiological functions of clathrin-mediated endocytosis. *Nature reviews. Molecular cell biology* **12**, 517-533
73. Saheki, Y., and De Camilli, P. (2012) Synaptic vesicle endocytosis. *Cold Spring Harbor perspectives in biology* **4**, a005645

74. Cosker, K. E., and Segal, R. A. (2014) Neuronal signaling through endocytosis. *Cold Spring Harbor perspectives in biology* **6**
75. Beattie, E. C., Carroll, R. C., Yu, X., Morishita, W., Yasuda, H., von Zastrow, M., and Malenka, R. C. (2000) Regulation of AMPA receptor endocytosis by a signaling mechanism shared with LTD. *Nature neuroscience* **3**, 1291-1300
76. Man, H. Y., Lin, J. W., Ju, W. H., Ahmadian, G., Liu, L., Becker, L. E., Sheng, M., and Wang, Y. T. (2000) Regulation of AMPA receptor-mediated synaptic transmission by clathrin-dependent receptor internalization. *Neuron* **25**, 649-662
77. Ahmadian, G., Ju, W., Liu, L., Wyszynski, M., Lee, S. H., Dunah, A. W., Taghibiglou, C., Wang, Y., Lu, J., Wong, T. P., Sheng, M., and Wang, Y. T. (2004) Tyrosine phosphorylation of GluR2 is required for insulin-stimulated AMPA receptor endocytosis and LTD. *The EMBO journal* **23**, 1040-1050
78. Brorson, J. R., Manzolillo, P. A., Gibbons, S. J., and Miller, R. J. (1995) AMPA receptor desensitization predicts the selective vulnerability of cerebellar Purkinje cells to excitotoxicity. *The Journal of neuroscience : the official journal of the Society for Neuroscience* **15**, 4515-4524
79. McDonald, J. W., Althomsons, S. P., Hyrc, K. L., Choi, D. W., and Goldberg, M. P. (1998) Oligodendrocytes from forebrain are highly vulnerable to AMPA/kainate receptor-mediated excitotoxicity. *Nature medicine* **4**, 291-297
80. Takei, K., Mundigl, O., Daniell, L., and De Camilli, P. (1996) The synaptic vesicle cycle: a single vesicle budding step involving clathrin and dynamin. *The Journal of cell biology* **133**, 1237-1250
81. Zhang, J. Z., Davletov, B. A., Sudhof, T. C., and Anderson, R. G. (1994) Synaptotagmin I is a high affinity receptor for clathrin AP-2: implications for membrane recycling. *Cell* **78**, 751-760
82. Granseth, B., Odermatt, B., Royle, S. J., and Lagnado, L. (2006) Clathrin-mediated endocytosis is the dominant mechanism of vesicle retrieval at hippocampal synapses. *Neuron* **51**, 773-786
83. Watanabe, S., Trimbuch, T., Camacho-Perez, M., Rost, B. R., Brokowski, B., Sohl-Kielczynski, B., Felies, A., Davis, M. W., Rosenmund, C., and Jorgensen, E. M. (2014) Clathrin regenerates synaptic vesicles from endosomes. *Nature* **515**, 228-233
84. Kundra, R., Ciryam, P., Morimoto, R. I., Dobson, C. M., and Vendruscolo, M. (2017) Protein homeostasis of a metastable subproteome associated with Alzheimer's disease. *Proceedings of the National Academy of Sciences of the United States of America* **114**, E5703-E5711
85. Ciryam, P., Kundra, R., Morimoto, R. I., Dobson, C. M., and Vendruscolo, M. (2015) Supersaturation is a major driving force for protein aggregation in neurodegenerative diseases. *Trends in pharmacological sciences* **36**, 72-77
86. Labbadia, J., and Morimoto, R. I. (2015) Repression of the Heat Shock Response Is a Programmed Event at the Onset of Reproduction. *Molecular cell* **59**, 639-650
87. Campeau, E., Ruhl, V. E., Rodier, F., Smith, C. L., Rahmberg, B. L., Fuss, J. O., Campisi, J., Yaswen, P., Cooper, P. K., and Kaufman, P. D. (2009) A versatile viral system for expression and depletion of proteins in mammalian cells. *PloS one* **4**, e6529
88. Hageman, J., and Kampinga, H. H. (2009) Computational analysis of the human HSPH/HSPA/DNAJ family and cloning of a human HSPH/HSPA/DNAJ expression library. *Cell stress & chaperones* **14**, 1-21
89. Jackson, S. J., Kerridge, C., Cooper, J., Cavallini, A., Falcon, B., Cella, C. V., Landi, A., Szekeres, P. G., Murray, T. K., Ahmed, Z., Goedert, M., Hutton, M., O'Neill, M. J., and Bose, S. (2016) Short Fibrils Constitute the Major Species of Seed-Competent Tau in the Brains of Mice Transgenic for Human P301S Tau. *The Journal of neuroscience : the official journal of the Society for Neuroscience* **36**, 762-772

**Figure legends:**

**Fig. 1. Tau inclusions sequester major cytosolic molecular chaperones of the HSP70 family.** HEK293 tau P301S cells were induced to express tau P301S mutant protein, and incubated with insoluble tau seeds. Tau inclusions were detected by immunostaining cells with PG5 (a, f and k) and MC1 antibodies (b, g and l) three days post seeding. Panel A, molecular chaperones in the cytosol were detected by immunofluorescence microscopy. The cellular localization of chaperones HSC70 (a-e) and inducible HSP70 (f-j, anti-HSP70/HSC70 antibody; k-n, anti-HSP70 antibody, clone 4G4) was examined in three cell populations: negative cells, MC1 positive (arrowheads) and PG5/MC1 positive (arrows) cells. The anti HSP70 antibody 4G4 is not compatible with MC1, thus co-staining was conducted only with PG5 and 4G4 antibodies. Constitutively expressed HSC70 and inducible HSP70 were sequestered to the PG5/MC1 positive tau inclusions (c, h and l, arrows), whereas sequestration was not observed in cells with dispersed/diffuse MC1 positive tau (c, h and l, arrowheads). The boxed areas (c, h and l) are enlarged to highlight the colocalization between PG5 positive tau aggregates and chaperones which appears yellow in the overlay (e, j and n). Images shown are maximal projections of a z-series of fluorescence confocal slices through the entire cell volume (scale bar, 10 μm) and are representative of three independent experiments. Panel B, colocalization of tau aggregates with chaperone indicated was quantified using Pearson's correlation coefficient (PCC). Individual cells were selected as regions of interest and analyzed using the Coloc2 plugin of the Fiji ImageJ software. Pearson's R value (above threshold) was measured per cell ($n \geq 25$) and dot plotted with mean and SD. P-values were determined using a two-tailed unpaired Student's t-test, **** $P<0.0001$.

**Fig. 2. Sequestration of other constitutive and inducible molecular chaperones by PG5 positive tau inclusions.** Tau inclusions were detected by immunostaining with PG5 and MC1 antibodies in tau P301S expressing cells three days post seeding to define three cell populations: negative cells, MC1 positive (arrowheads) and PG5/MC1 positive

(arrows) cells. Panel A, cellular localization of other major constitutively expressed chaperones and co-chaperones such as DNAJB1 (a-e), HSP90β (f-j) and HSP110 (k-o) was examined. Panel B, cellular localization of the inducible chaperones HSP27 (p-t) and HSP90α (u-y) was examined. Cells exhibiting only MC1 staining do not exhibit sequestration of chaperones (arrowheads), whereas constitutive and inducible chaperones are sequestered by tau inclusions (arrows). The overlay between tau aggregates and chaperones in the boxed area is enlarged and displays colocalization as yellow colored overlay (e, j, o, t and y). Images shown are representative of three independent experiments. Scale bar, 10 μm.

**Fig. 3. Inhibition of clathrin-mediated endocytosis by tau aggregate species in both PG5 and MC1 positive cells.** HEK293 tau P301S cells were induced to express tau P301S mutant protein, and transferrin uptake was assayed at day 3 post seeding. Cells were stained with pathological tau specific PG5 and MC1 antibodies (a-d) or total tau antibody HT7 (e-h). Panels a-d show inhibition of transferrin uptake in cells stained with PG5 (c, arrows) and/or MC1 (c, arrowheads). (e-h), tau protein aggregation but not overexpression of total tau protein detected by HT7 (f, arrows) leads to the inhibition of clathrin-mediated endocytosis (g, arrows). Scale bar, 10 μm. Panel i shows quantification of transferrin uptake as measured by the sum fluorescence intensities per cell in three cell populations. Shown are the mean values of individual cells with error bars representing S.D. P-values were determined using a two-tailed Student's t-test, **** $P<0.0001$.

**Fig. 4. Aggregation and sequestration of the luciferase folding sensor by PG5-positive tau inclusions.** Panel A, HEK293 tau P301S cells were infected with lentivirus encoding EGFP (a-d) or firefly Luciferase DM-EGFP folding sensor (e-h). Cells were induced with tetracycline to express both tau P301S and fLucDM-EGFP proteins and subsequently incubated with sarkosyl-insoluble tau seeds. Three days following seeding, cells were immunostained to identify MC1 (b and f, arrowheads) and PG5/MC1 (a and e, arrows) positive cells and to examine for the subcellular localization of the luciferase folding sensor (c and g). PG5-positive tau inclusions sequester fLucDM-EGFP (g, arrows)

but not EGFP proteins (c, arrows) indicating the changing cellular folding capacity for conformationally challenged proteins. Scale bar, 10 μm. Panel B, PG5-positive tau inclusions sequester fLucDM-EGFP (k is the overlay image of e and g, the boxed area are enlarged in panel l to highlight the colocalization), but not EGFP proteins (i, enlarged in j) indicating the changing cellular folding capacity for conformationally challenged proteins. Panel C, colocalization of between tau species and fLucDM-EGFP was quantified using Pearson correlation coefficient (PCC). Pearson's R value (above threshold) was measured per cell ($n \geqslant 25$) and presented as a dot plot with mean and S.D. P-values were determined using a two-tailed unpaired Student's t-test, ** $P<0.01$, **** $P<0.0001$.

**Fig. 5. Restoration of proteostasis by small molecule proteostasis regulators.** (a-p), HEK293 tau P301S cells were induced to express mutant tau protein and seeded with insoluble tau seed. Two days post seeding, the cells were treated with small molecule proteostasis regulators (A3, C1 and F1) at indicated concentrations for additional 24 hours. Transferrin uptake was assayed before cells were fixed and immunostained. Transferrin uptake (c, g, k and o) in DMSO (a-d), A3 (e-h), C1 (i-l) and F1 (m-p) are shown in cell populations stained by pathological tau specific PG5 (a, e, i and m, arrows) and MC1 (b, f, j and n, arrowheads) antibodies. Scale bar, 10 μm. (q), quantification of transferrin uptake in three cell populations treated with A3, C1, and F1.

**Fig. 6. Restoration of clathrin-mediated endocytosis by tunable expression of HSC70.** (A-B), HEK293 tau P301S cell line stably expressing V5-tagged HSC70 under the control of the cumate responding promoter was established. The induction of V5 tagged HSC70 upon cumate treatment was confirmed by staining with anti-V5 antibody with HEK293 tau P301S cell line with (c and d) or without cumate (a and b) and by the increased level of total HSC70/HSP70 (e-h). Scale bar, 10 μm. (C), HEK293 tau P301S-V5 HSC70 cells were seeded with insoluble tau. Two days post seeding, cells were treated with or without cumate for an additional 24 hours. Transferrin uptake in the cell population stained by pathological tau specific PG5 and MC1 antibodies was quantified as described.

**Fig. 7. Reduced sequestration of luciferase folding sensor by small molecule proteostasis regulator in tau inclusion expressing cells.** HEK293 tau P301S-fLucDM-EGFP cells were induced with tetracycline to express both tau P301S and fLucDM-EGFP proteins, and were then incubated with sarkosyl-insoluble tau seeds. Two days post seeding, the cells were treated with DMSO (a-e) or the small molecule proteostasis regulator A3 (f-j) at 10 μM for an additional 24 hours. Cells were immunostained to identify PG5 positive cells (a and f, arrows) and to examine the subcellular localization of the luciferase folding sensor (b and g). The boxed areas in the superimposed images between PG5 and fLucDM-EGFP (c and h) are enlarged to show colocalization between PG5 positive tau aggregates and chaperones, which appears yellow in the overlay (e and j). Images are maximal projections of a z-series of fluorescence confocal slices through the entire cell volume (scale bar, 10 μm) and are representative of three independent experiments. (k), colocalization between tau species and fLucDM-EGFP was quantified using Pearson correlation coefficient (PCC). Pearson's R value (above threshold) was measured per cell ($n \geqslant 40$) and presented as a dot plot with mean and S.D. P-values were determined using a two-tailed unpaired Student's t-test, * $P<0.1$, **** $P<0.0001$.

Fig. 1

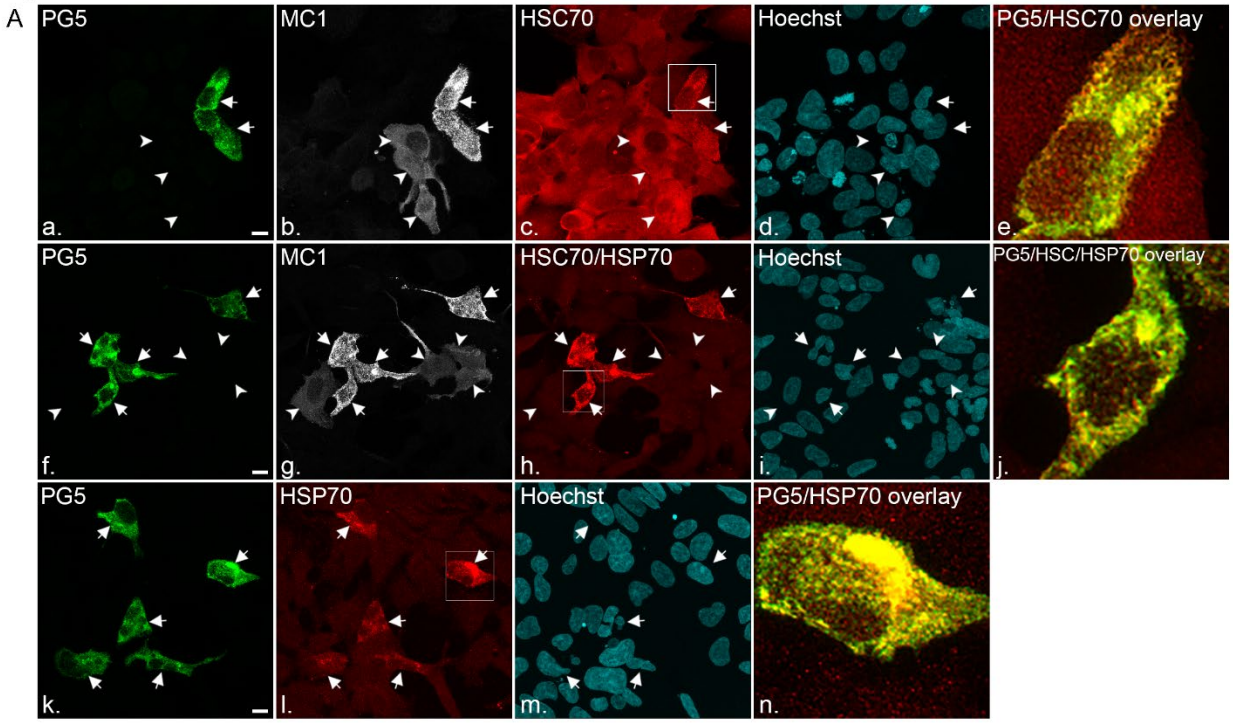


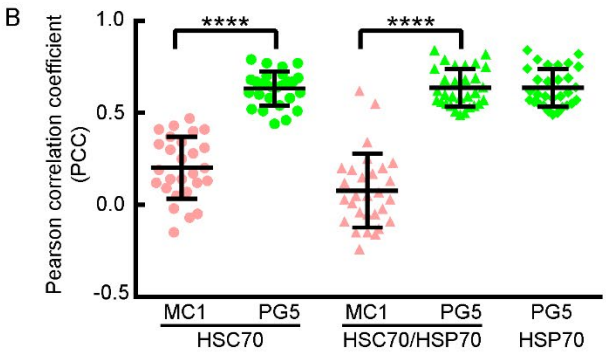

Fig. 2

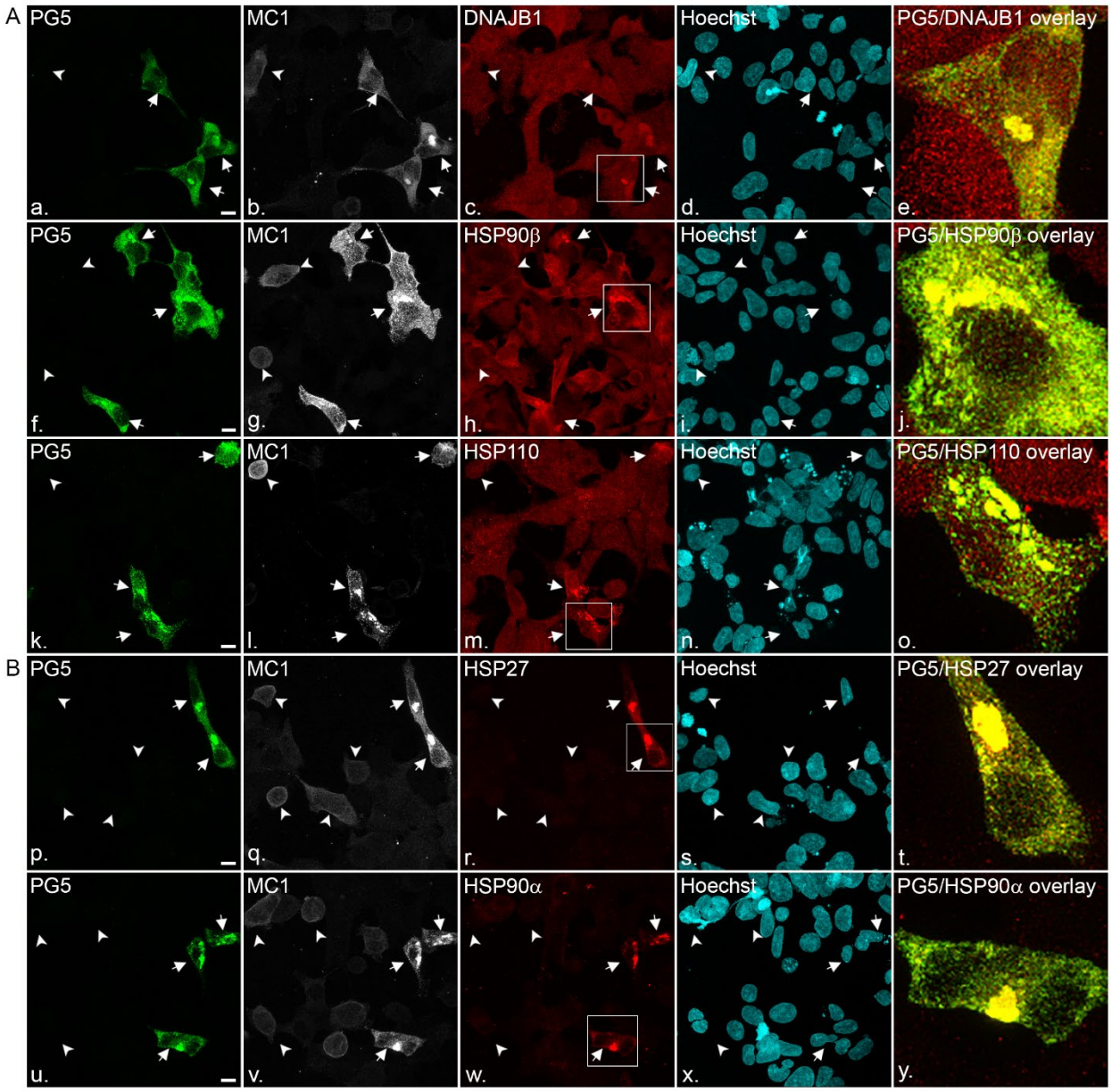

Fig. 3

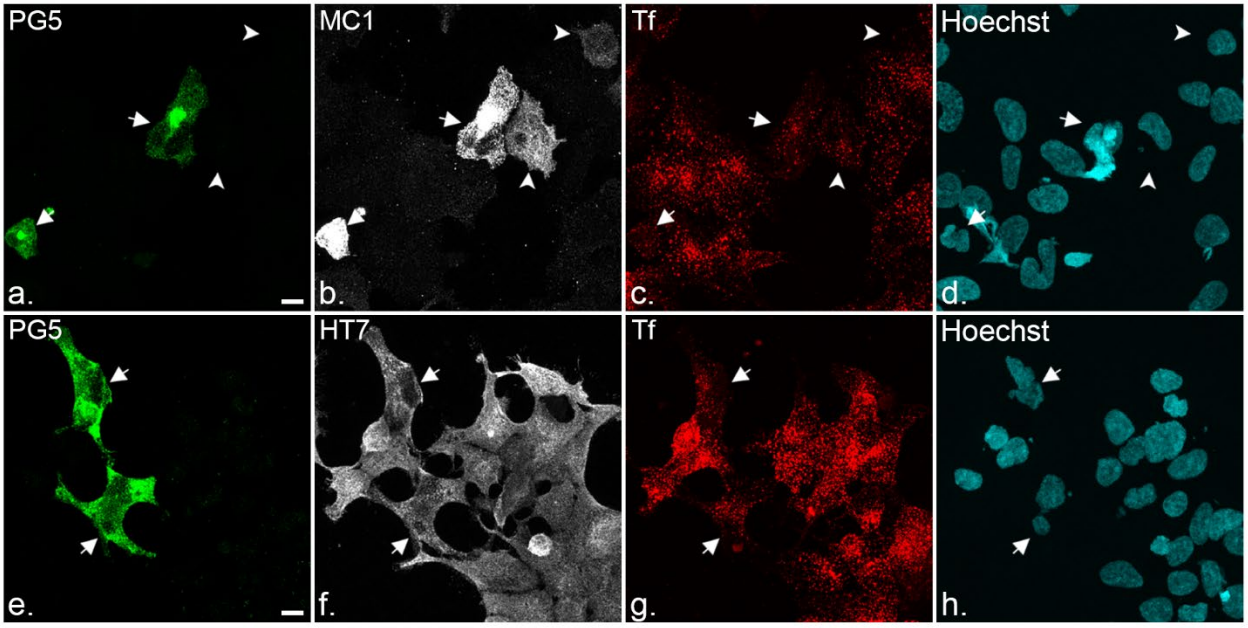


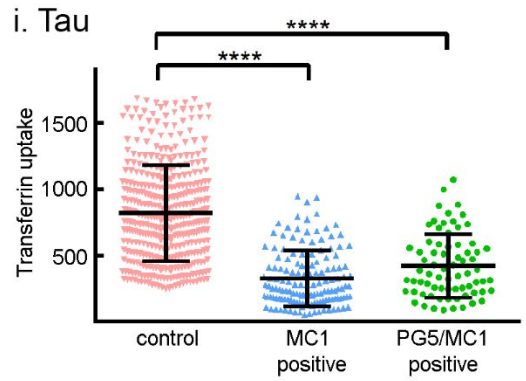

Fig. 4

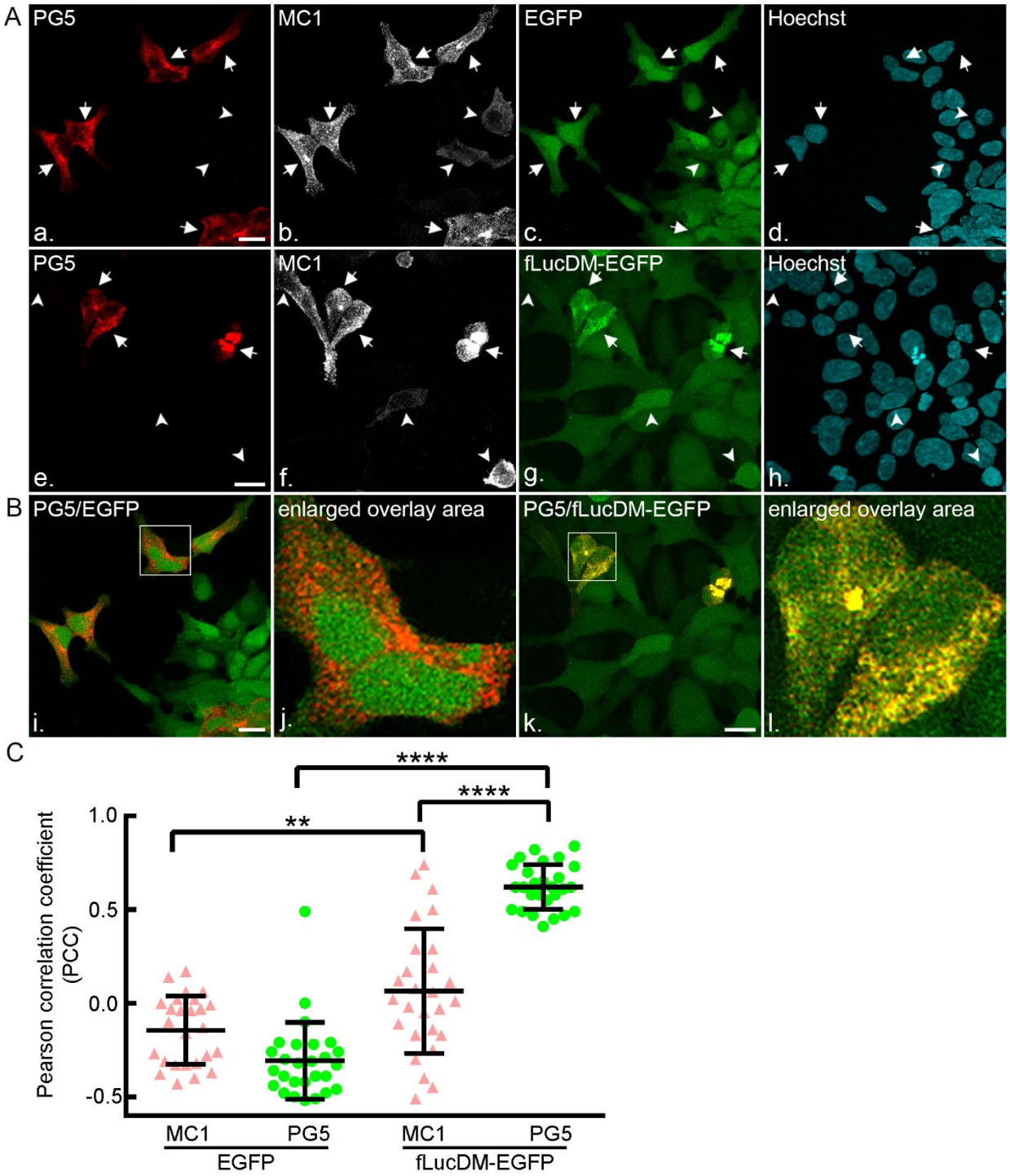

Fig. 5

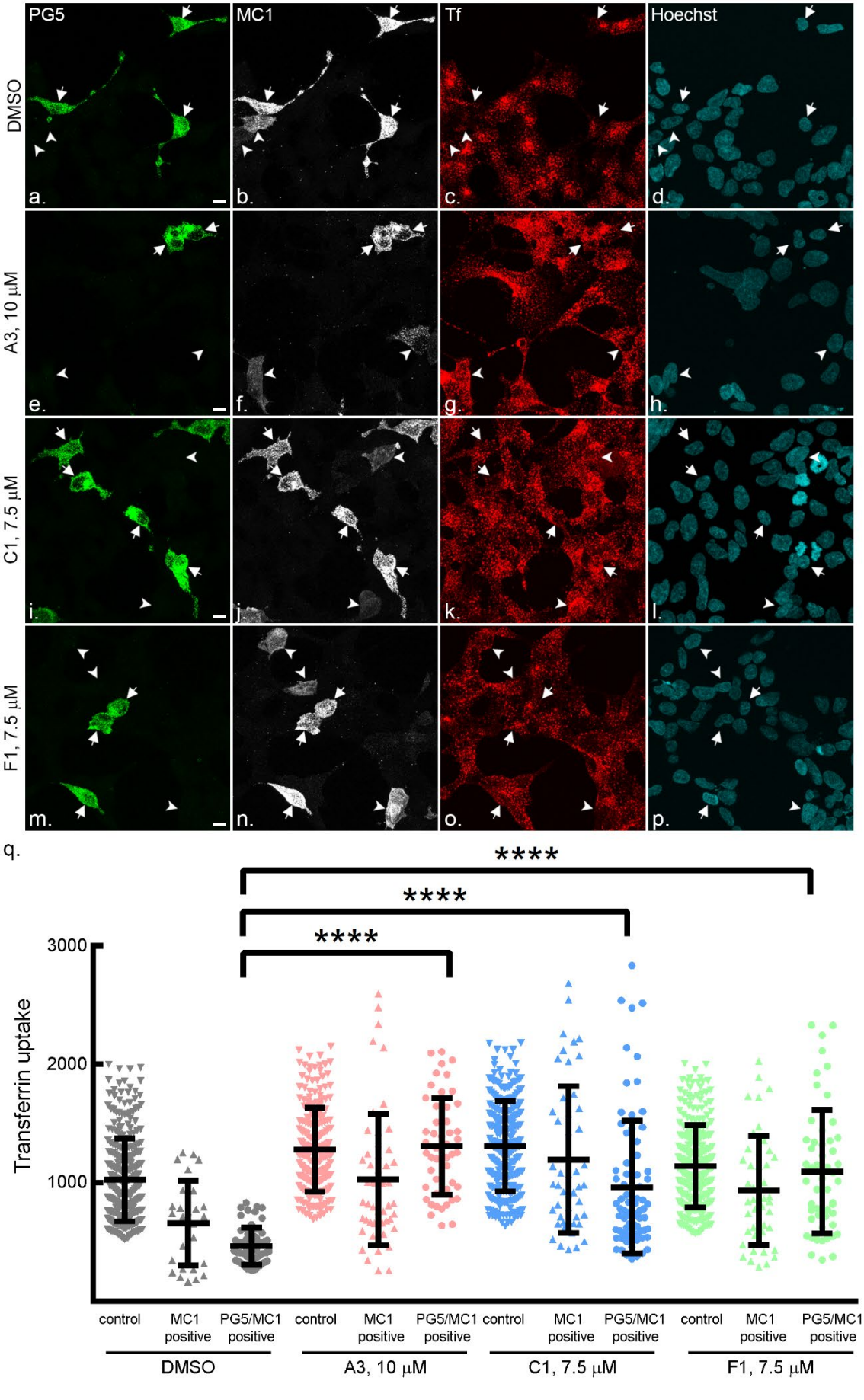

Fig. 6

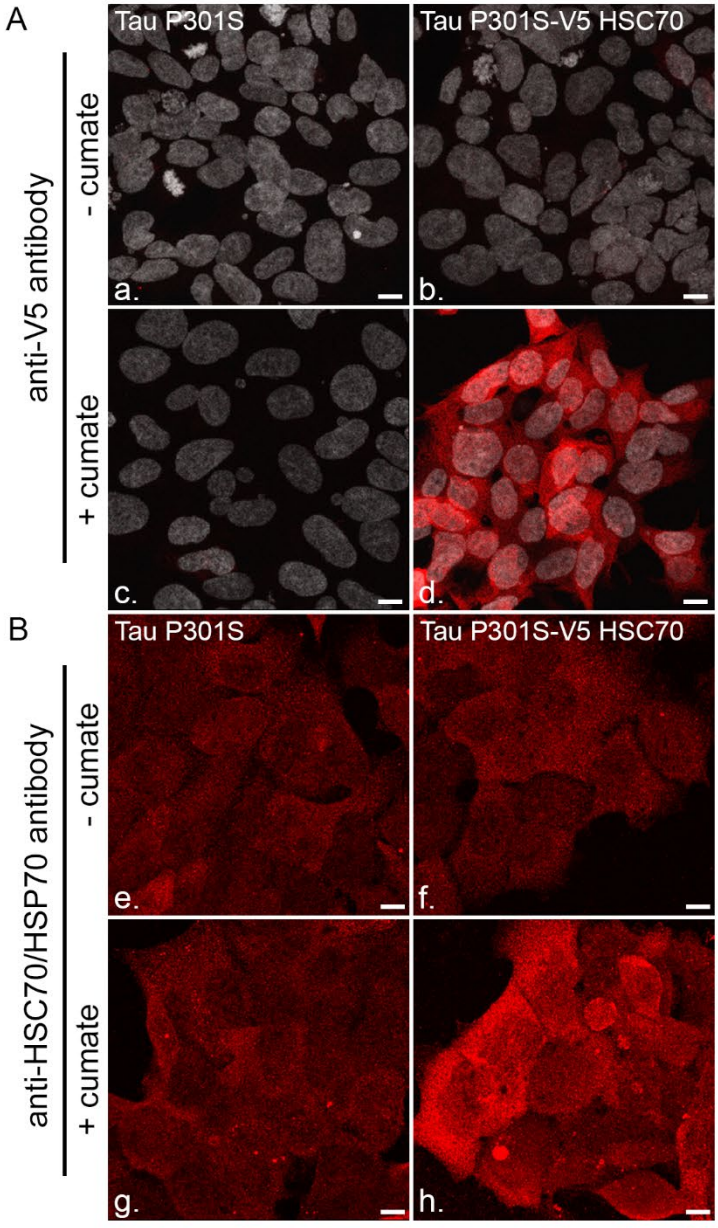


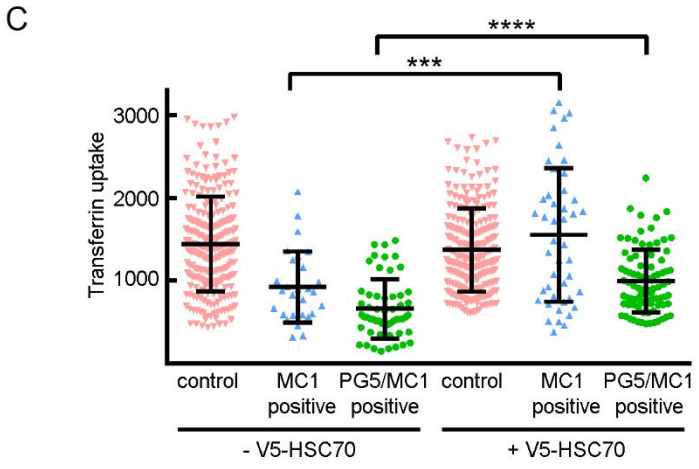

Fig. 7

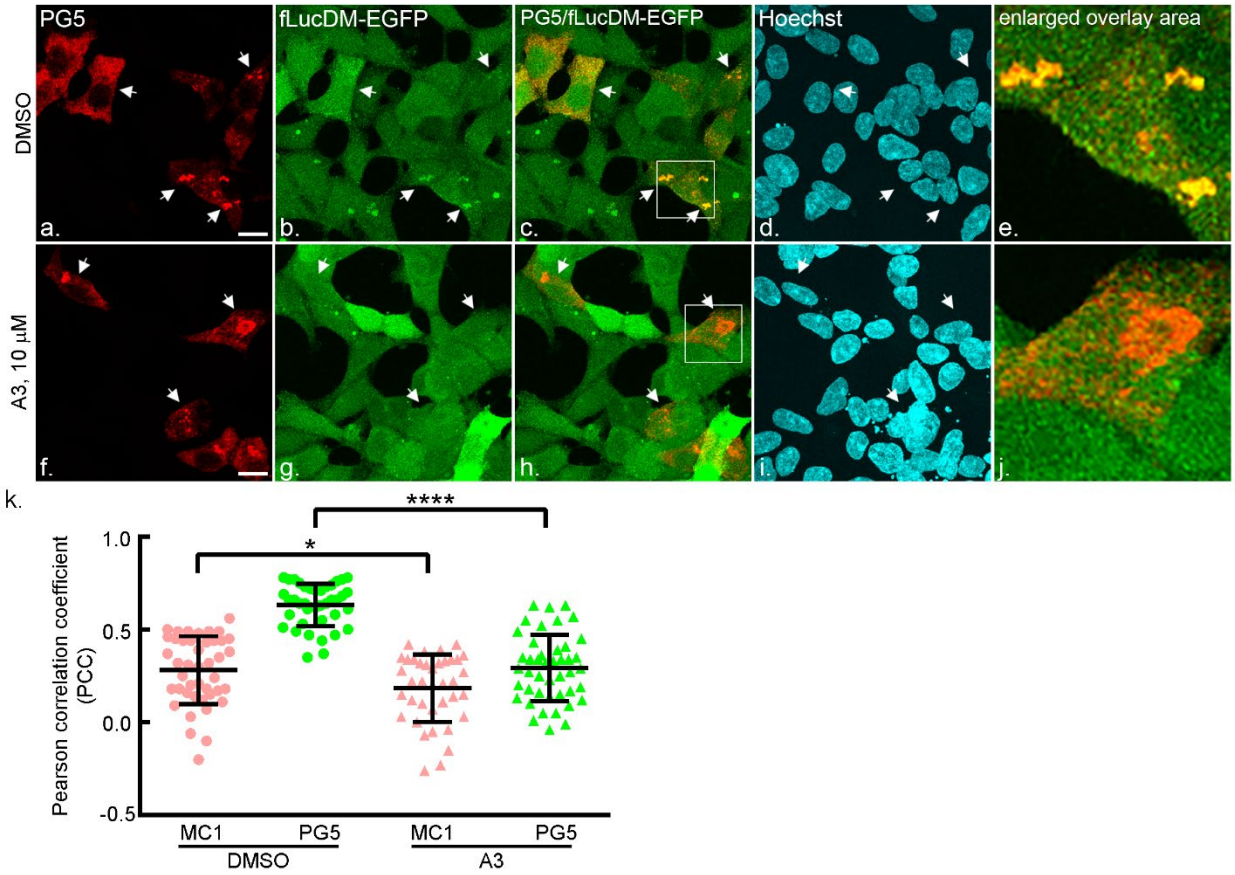

# Tau protein aggregates inhibit the protein-folding and vesicular trafficking arms of the cellular proteostasis network

Anan Yu, Susan G. Fox, Annalisa Cavallini, Caroline Kerridge, Michael J. O'Neill, Joanna Wolak, Suchira Bose and Richard I. Morimoto

*J. Biol. Chem. published online April 1, 2019*

---

Access the most updated version of this article at doi: 10.1074/jbc.RA119.007527